Insertion and Pore Formation Driven by Adsorption of Proteins Onto Lipid Bilayer Membrane–Water Interfaces

Martin J. Zuckermann*† and Thomas Heimburg*‡

*MEMPHYS Group, Department of Chemistry, Technical University of Denmark, DK-2800 Lyngby, Denmark, †School of Physics, University of New South Wales, Sydney 2052, Australia, and ‡Membrane Thermodynamics Group, Max-Planck-Institute for Biophysical Chemistry, 37077 Göttingen, Germany

ABSTRACT We describe the binding of proteins to lipid bilayers in the case for which binding can occur either by adsorption to the lipid bilayer membrane–water interface or by direct insertion into the bilayer itself. We examine in particular the case when the insertion and pore formation are driven by the adsorption process using scaled particle theory. The adsorbed proteins form a two-dimensional "surface gas" at the lipid bilayer membrane–water interface that exerts a lateral pressure on the lipid bilayer membrane. Under conditions of strong intrinsic binding and a high degree of interfacial converge, this pressure can become high enough to overcome the energy barrier for protein insertion. Under these conditions, a subtle equilibrium exists between the adsorbed and inserted proteins. We propose that this provides a control mechanism for reversible insertion and pore formation of proteins such as melittin and magainin. Next, we discuss experimental data for the binding isotherms of cytochrome *c* to charged lipid membranes in the light of our theory and predict that cytochrome *c* inserts into charged lipid bilayers at low ionic strength. This prediction is supported by titration calorimetry results that are reported here. We were furthermore able to describe the observed binding isotherms of the pore-forming peptides endotoxin (α5-helix) and of pardaxin to zwitterionic vesicles from our theory by assuming adsorption/insertion equilibrium.

INTRODUCTION

The adsorption of proteins and peptides to lipid bilayers is, in general, due to a combination of electrostatic interactions with the polar heads of anionic lipid molecules and hydrophobic interactions with the lipid acyl chains. The set of adsorbed proteins can then form a two-dimensional (2D) gas at the lipid bilayer interface, which exerts a lateral pressure on the membrane itself. This will be referred to as the "surface gas." Heimburg and Marsh (1995) treated the case of binding of cytochrome *c* to charged lipid membranes and have shown that this is the case by deriving and fitting theoretical expressions, which allow the adsorbed proteins or peptides to form such a surface gas. Their analysis took account of both the electrostatic interactions between proteins and anionic lipids and van der Waals interactions between adsorbed proteins. The concentration of the adsorbed proteins was found to be much lower than that calculated for the case of Langmuir absorption. This implies that the binding isotherms are in no way classical Langmuir isotherms, which require well-defined binding sites for the adsorbants, but rather Gibbs isotherms, which describe the case of laterally mobile adsorbed molecules.

It was found that some species of adsorbed proteins or peptides insert in such a way as to form pores at a sufficiently high adsorbate concentration (Ladokhin et al., 1997; Bechinger, 1999; Shai, 1999). Furthermore, many of these inserting species aggregated to form oligomeric pores. In his recent review article, Shai (1999) considers the case of amphipathic membrane lytic peptides with an α-helical structure and identifies two mechanisms for the association of these peptides with lipid membranes. In the first mechanism, the peptides adsorb to the lipid bilayer–water interface by binding preferentially to the polar heads of the lipid molecules. They do not insert into the bilayer, but associate to form localized "carpets" at high surface coverages. This is assumed to give rise to a change in bilayer curvature that would lead to lysis. Shai proposes that this mechanism describes the adsorption of certain target-specific antimicrobial peptides such as cecropin B and dermaseptin B to lipid bilayers, and that it is electrostatically driven, involving the positive charges on the peptide backbone and the presence of anionic lipids in the bilayer. In contrast, Shai points out that several cell nonselective membrane–lytic amphipathic peptides (MLAPs) such as pardaxin and the α5-helix of δ-endotoxin first adsorb on the lipid bilayer–water interface at low concentrations and then form oligomeric transbilayer pores above a specific adsorbate concentration. He further proposed that the pores resemble "barrel staves," i.e., they would then be composed of a fixed number of proteins with their hydrophilic residues inside the pore and their hydrophobic residues in direct contact with the acyl chains of the bilayer lipids. Barrel staves pores have also been conjectured to be formed by toxins (Ojcius and Young, 1991) and certain drugs such as poly-enes (Hartsel et al., 1993). The

Received for publication 28 November 2000 and in final form 16 August 2001.

M. J. Zuckermann's E-mail is martinz@sfu.ca.

Address reprint requests to Thomas Heimburg, Max-Planck-Inst./Biophys. Chem., Membrane Thermodynamics Group, AG012, Am Fassberg 11, D-37077 Göttingen, Germany. Tel.: +49-551-201-1412; Fax: +49-551-201-1501; E-mail: theimbu@gwdg.de.

0006-3495/01/11/2458/15 $2.00

formation of the barrel staves considered by Shai are driven by hydrophobic rather then electrostatic interactions, implying that they would be stabilized by hydrophobic interactions between the peptide components and the lipid acyl chains and, in some cases, membrane-bound sterols. Other pore-forming peptides include alamethicin, melittin (Ladokhin et al., 1997), and magainin (Bechinger, 1999; Yang et al., 2000). Experimental results indicate that alamethicin pores consist of oligomers with a finite number of peptides in the range of 6–11 (Gennis, 1989), whereas melittin and the nonspecific amphipathic peptides may well form pores composed of an increasing number of monomers as its concentration increases (Ladokhin et al., 1997; Shai, 1999).

The reversible control of protein and peptide insertion is of considerable relevance for biological membranes because it provides a means for altering membrane function. Our particular interest is to derive a theoretical model for the general case when such molecules can both adsorb onto the lipid bilayer–water interface and insert into the hydrophobic core of the lipid bilayer with the possibility of aggregation and pore formation. This theory will then be applied to understand the binding and insertion of MLAPs into small unilamellar lipid vesicles and to investigate the possibility that cytochrome *c* inserts into lipid bilayers at a high enough concentration. The value of this concentration is strongly dependent on the edge tension of the inserted protein or peptide in the bilayer. Here the edge tension is defined as the energy per unit circumference of the inserted protein or peptide in the lipid bilayer (Dan and Safran, 1998). The adsorbed proteins can then begin to insert in a reversible manner as integral proteins grouping together to form aqueous pores. To examine this situation in detail, we study the case of competition between adsorption and insertion, and the influence of a second adsorbing species on the insertion by extending a theory by Minton (1999) for the effect of multiple adsorbate configurations on the adsorption of globular proteins on locally planar surfaces. The use of this theory ensures that the inserted and adsorbed proteins are self-avoiding, and, therefore, that the latter can never lie on top of the former.

In Minton's theory, binding isotherms are derived by assuming that the proteins are hard rectangular prisms that can bind on the interface in either side-on configurations with their long axes parallel to the bilayer plane or end-on configurations with their long axes perpendicular to the bilayer plane. Minton also proposed that the adsorbed proteins could form oligomers or *m*-mers with *m* monomers in the end-on configuration forming a close-packed rectangular prism, i.e., they can bind in different orientations. Minton's expressions for the adsorption activity coefficients were obtained from a relation by Talbot et al. (1994) for a mixture of hard convex particles in two-dimensions, which was derived using scaled particle theory. The rectangular and square areas of contact (footprints) of the related prisms then correspond to Talbot's hard convex particles. In our generalization, we examine the case where the adsorbed proteins are able to coexist with the inserted species. Hence, we take the side-on configuration to represent an adsorbed protein, and the end-on configuration of a single protein represents the inserted species. This requires that the total surface area is no longer constant but depends on the end-on footprint area and the number of inserted proteins. The pores are a generalization of the *m*-mers, again inserted, and it is easy to include a second adsorbing species by adding a third equilibrium constant in the appropriate manner. Because Minton's general expressions can be used for any shape, it is also straightforward to consider the proteins as cylindrical instead of prismatically shaped.

The detailed expressions for isotherms describing insertion and pore formation as driven by adsorption are derived in the Theory section. The expressions for the isotherms cannot be solved analytically and therefore require numerical solution. The Results are presented in the next section for all cases. This section further describes how our theoretical analysis can be used to understand data from both binding studies and simultaneous electron spin resonance (ESR) experiments for the binding of cytochrome *c* to dioleoyl phosphatidylglycerol (DOPG) lipid bilayers (Heimburg and Marsh, 1995; Heimburg et al., 1999). We also report and discuss measurements of binding isotherms of cytochrome *c* to DOPG bilayers using isothermal titration calorimetry. Finally, we use the analysis presented in the Theory section to examine the observed binding isotherms of an endotoxin helix and of pardaxin, which are both pore-forming peptides. The last section contains a discussion of the results.

MATERIALS AND METHODS

Horse heart cytochrome *c* (type VI) was purchased from Sigma Chemical Co. (St. Louis, MO). DOPG (Avanti Polar Lipids, Birmingham, AL) was used without further purification. All lipid dispersions and protein solutions for titration calorimetry were prepared in a 2-mM HEPES, 1-mM EDTA buffer at various NaCl concentrations. The sodium concentrations, given in Fig. 7, are the sum of the NaCl concentration, the counterions of HEPES and EDTA and the NaOH-concentration used to adjust the pH. The pH of 7.5 was carefully adjusted in both lipid and protein solutions to avoid heats of protonation.

Titration calorimetry was performed on a MicroCal, Inc. Isothermal titration unit (Omega cell) (cf. Heimburg and Biltonen, 1994). The protein solution (1.61 mM cytochrome *c*) was titrated in 10-μl steps during 20 s to the lipid dispersion (0.536 mM DOPG), using a rotating syringe (400 rpm). The cell volume was 1.37 ml. Experiments were performed at 16°C.

THEORY

In this section, we refer to the adsorbing and inserting proteins (peptides) as ligands. We now derive expressions for the equilibrium isotherms for ligands that can both adsorb on the lipid bilayer–water interface and insert into

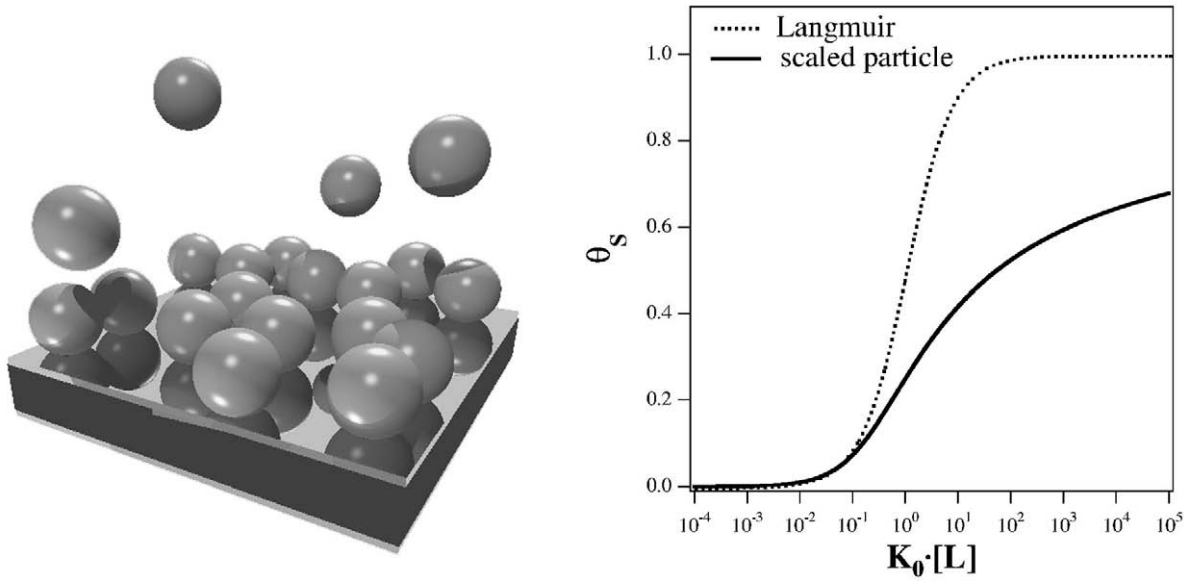

FIGURE 1 *Left*: Binding of spherical ligands to a flat surface. *Right*: Langmuir isotherm compared to scaled particle isotherm for ligands with hard disc cross section. The two isotherms differ significantly above a surface coverage of 10% ($\theta_S = 0.1$).

the bilayer either as single ligands or pores composed of several ligands.

We begin by giving an overview of equilibrium isotherms for ligands in a bulk solution binding onto a planer boundary. The basic scheme for binding of ligands to flat surfaces is shown in Fig. 1 (*left*). The ligands are represented as hard spheres randomly arranged on this surface. The Langmuir isotherm is often used to describe such binding, and it is given by

$$K_0[L] = \frac{\theta}{1-\theta}. \quad (1)$$

Here, θ is the fraction of binding sites occupied by adsorbed ligands, K_0 is the equilibrium binding constant and $[L]$ is the bulk concentration of ligands in solution. The Langmuir isotherm of Eq. 1 describes the binding of ligands to spatially fixed independent and identical binding sites. It has been used to analyze the binding of identical ligands to macromolecules, e.g., for oxygen binding to hemoglobin. In this case, the number of free sites available for binding is simply the total number of sites less the number of occupied sites. This situation does not apply to lipid bilayers where the number of available sites is modulated by hard core repulsion between the ligands, because this requires that the excluded volume of the adsorbed ligands must be included in the formalism. Under these circumstances, the accessible free surface is significantly smaller than the total surface less the occupied surface. The ligands generally do not bind onto interfacial areas already occupied by other ligands. In a 2D formulation of this problem, we are thus required to take account of the footprint (effective excluded area) of the adsorbed ligand in determining the interfacial area of the available binding sites. This situation was analyzed by Chatelier and Minton (1996), who treated the footprint as a hard convex 2D particle with a given shape and then used scaled particle theory (SPT) to describe the surface gas formed by the ensemble of adsorbed ligands. In this way, they derived a realistic Gibbs adsorption isotherm, which is given in the equation,

$$K_0[L] = \left(\frac{\theta}{1-\theta}\right)\exp\left(\frac{\theta}{1-\theta} - \epsilon + \frac{\epsilon}{(1-\theta)^2}\right). \quad (2)$$

Here, ϵ depends on the shape of the convex particle and takes on values of unity for a circle and $4/\pi$ for a rectangle with an axial ratio of four. The Langmuir and Gibbs isotherms are compared in Fig. 1 for the same binding parameters. This figure shows that the adsorption is significantly suppressed at high ligand concentrations in the case of the Gibbs isotherm as compared to the Langmuir isotherm, indicating the considerable effect of the large lateral pressures of the surface gas formed by the adsorbate.

In the theory of Chatelier and Minton (1996), the ligands only bind to lipid bilayers by interfacial adsorption. Our object is to describe the binding of ligands to lipid bilayers in the case when binding can occur either by adsorption onto the interface or by direct insertion into the bilayer itself either in the form of single ligands or as pores formed from a finite number of ligands. In particular, we examine the case when two ligands competitively adsorb onto the interface but only one of them can also insert into the membrane. We then make the reasonable assumption that free ligands cannot adsorb onto either previously adsorbed or inserted ligands (see also above). We therefore require an extension

of Chatelier and Minton's theory that allows for several mutually exclusive configurations whose footprints are again represented by hard 2D convex particles. By configuration, we mean either different orientations of different degrees of aggregation. To this purpose, we first describe and then adapt a theory recently published by Minton (1999), which extends the result of Chatelier and Minton (1996) to the case when the ligands could present several configurations to the adsorbing surface. Examples of this situation are given in the Introduction and below.

Minton considered a finite number, M, of possible adsorbate configurations where the equation for the adsorption isotherm of the nth configuration ($n = 1, 2, \ldots, M$) is given by

$$K_n[L] = \tau_n \rho_n. \tag{3}$$

Here, K_n is the intrinsic equilibrium constant for the partitioning of ligand between the solution and the nth adsorbate configuration of the ligand, and ρ_n is the related number of ligands per unit area. τ_n is the activity coefficient of the nth adsorbate configuration and is based on an SPT expression due to Talbot et al. (1994) (see Introduction):

$$\tau_n = -\ln(1 - \langle \rho a \rangle) + \frac{A_n \langle \rho \rangle + s_n \langle \rho s \rangle / 2\pi}{1 - \langle \rho a \rangle} + \frac{A_n}{4\pi}\left[\frac{\langle \rho s \rangle}{1 - \langle \rho a \rangle}\right]^2, \tag{4}$$

where $\langle \rho \rangle = \sum_{n=1}^{M} \rho_n$, $\langle \rho a \rangle = \sum_{n=1}^{M} \rho_n A_n$, and $\langle \rho s \rangle = \sum_{n=1}^{M} \rho_n s_n$. Here, A_n is the area of the footprint of the nth adsorbate configuration, and s_n is its circumference. It is important to note that Talbot's original expression was derived for a mixture of hard convex particles on a planar surface, and, therefore, the M adsorbate species can also represent the ensemble of adsorbate configurations of several ligands.

We next extend Minton's theory as given in Eqs. 3 and 4 to the most general case that we wish to examine, that of two bound ligands, both of which can adsorb but only one can insert. The ligands are taken to have either a cylindrical or a rectangular prismatic shape. Adsorbed ligands are assumed to lie in the side-on configuration on the interface with their long axes parallel to the bilayer plane. The adsorption footprint for both shapes is then a rectangle. In contrast, inserted ligands are taken to lie in an end-on configuration with their long axes perpendicular to the bilayer plane. Their footprint is then either a circle or a square. Our model consists of ligands (proteins) in solution that adsorb in a side-on configuration, S, on the surface and can collectively insert into the bilayer to form pores, I, each composed of m single ligands in the presence of a second purely adsorbing species, S', which does not insert. This gives three binding species ($M = 3$) with $n = S, S', I$. Following Minton, we define Φ_n as the ratio of the fraction of the surface area occupied by the nth adsorbed or inserted species and the total interfacial area, A_T, of the bilayer. Then, ρ_n is given by

$$\rho_n = \frac{\Phi_n}{A_n}. \tag{5}$$

In Minton's case, the total interfacial area is constant, whereas in our case, A_T increases with the number of inserted pores, N_I, as

$$A_T = N_B A_B + N_I A_I, \tag{6}$$

where A_B is the reference site area and $N_B A_B$ is the total lipid surface area. N_B corresponds to a number of sites on the lipid surface. A_I is the cross-sectional areas of a pore. Let N_S, A_S and $N_{S'}$, $A_{S'}$ be the number and footprint area of adsorbed molecules of species S and S', respectively. Then, from Eqs. 5 and 6, Φ_S, $\Phi_{S'}$, and Φ_I can be written

$$\Phi_S = \frac{\theta_S a_S}{a_B + \theta_I}, \quad \Phi_{S'} = \frac{\theta_{S'} a_{S'}}{a_B + \theta_I}, \quad \Phi_I = \frac{\theta_I}{a_B + \theta_I}, \tag{7}$$

where θ_n and a_n ($n = S, S'$), a_B, and θ_I are given by

$$\theta_n = \frac{N_n}{N_B} \quad \theta_I = \frac{N_I}{N_B} \quad a_n = \frac{A_n}{A_I} \quad a_B = \frac{A_B}{A_I}. \tag{8}$$

We now give the following expressions for the isotherms in terms of θ_n, $n = S, S'$ and θ_I as derived from Eqs. 3–8. This derivation includes an additional term related to the edge tension opposing or favoring insertion of the pore into the lipid bilayer (Shillcock and Boal, 1996). For the adsorbed ligands, we obtain, taking $a_{S'} = a_S$ without loss of generality,

$$\theta_n = \frac{a_B}{a_S}\left[\frac{K_S(\theta_n, \theta_I)[L_n]}{1 + K_S(\theta_n, \theta_I)[L_n]}\right]. \tag{9}$$

Here, $[L_n]$ is the bulk concentration of species n, and the effective equilibrium constant, K_S, for adsorption onto the interface is given by

$$K_S(\theta_n, \theta_I) = K_0 \exp\left[-\frac{a'_S\theta + a'_{SI}\theta_I}{a_B - a_S\theta} - \left(\frac{b_S\theta + b_I\theta_I}{a_B - a_S\theta}\right)^2\right], \tag{10}$$

where $\theta = \theta_S + \theta'_S$. For the inserted pores, we obtain the isotherm equations,

$$\theta_I = K_I(\theta_n, \theta_I)[L_S]^m(a_B - a_S\theta). \tag{11}$$

Note that only $[L_S]$ appears on the right-hand side of this equation because S is the species that inserts. The effective equilibrium constant, K_I, for insertion is given by

$$K_I(\theta_n, \theta_I) = K_0^m \exp\left(-\frac{2\Gamma D_I}{kT}\right) \times \exp\left[-\frac{a''_{SI}\theta + a'_I\theta_I}{a_B - a_S\theta} - \left(\frac{c_S\theta + c_I\theta_I}{a_B - a_S\theta}\right)^2\right], \tag{12}$$

TABLE 1 General expressions in Eq. 10 and 12

Parameter	General Expression*
a'_S	$a_S+D_S^2/(2\pi A_I)$
a'_{SI}	$a_S + D_S D_I/(2\pi A_I)$
b_S	$[A_S D_S^2/(4\pi A_I^2)]^{1/2}$
b_I	$[A_S D_I^2/(4\pi A_I^2)]^{1/2}$
a''_{SI}	$1 + D_S D_I/(2\pi A_I)$
α'_I	$1 + D_S^2/(2\pi A_I)$
c_S	$D_S/(2\pi A_I)^{1/2}$
c_I	$D_I/(2\pi A_I)^{1/2}$

*A_S and D_S are the footprint area and circumference, respectively, for the adsorbed ligand, whereas A_I and D_I are the footprint area and circumference, respectively, for the inserted ligand (pore). a_S is defined in Eq. 8.

TABLE 2 Expressions in Eq. 10 and 12 for three specific shapes: rectangular prisms; cylinders, and pores, calculated from the general expressions in Table 1

Parameter	Rectangular* Prism	Cylinder† (Pore)	Sphere‡
A_S	La^2	$4Lr^2$	πr^2
A_I	a^2	$\pi r^2 s^2(m)$	πr^2
A_B	La^2	$4Lr^2$	πr^2
D_S	$2(1 + L)a$	$4(1 + L)r$	$2\pi r$
D_I	$4a$	$2\pi r s(m)$	$2\pi r$
a_B	L	$L/s^2(m)$	1
a_S	L	$4L/(\pi s^2(m))$	1
a'_S	$L + 2(1 + L)^2/\pi$	$4[L + 2(1 + L)^2/\pi]/\pi s^2(m)$	3
a'_{SI}	$L + 4(1 + L)/\pi$	$4[L/s(m) + (1 + L)]/\pi s(m)$	3
b_S	$(1 + L)(L/\pi)^{1/2}$	$4L^{1/2}(1 + L)/\pi^{3/2}s^2(m)$	1
b_I	$2(L/\pi)^{1/2}$	$2L^{1/2}/\pi^{1/2}s(m)$	1
a''_{SI}	$1 + 4(1 + L)/\pi$	$1 + 4(1 + L)/\pi s(m)$	3
a'_I	$1 + 8/\pi$	3	3
c_S	$(1 + L)/\pi^{1/2}$	$2(1 + L)/\pi s(m)$	1
c_I	$2/\pi^{1/2}$	1	1
$s(m)_{Pore}$		$(1 + \sin(\pi/m))/\sin(\pi/m)$	
$s(m)_{aggregate}$§		$m^{1/2}$	

*For the rectangular prismatic configuration of the ligand, L is the height and a is the edge length of the square base.
†For the cylindrical configuration, L is the height, r is the radius of the circular base for a single ligand, and $s(m)$ is the circumference of a pore composed of m ligands.
‡The cytochrome c case, where adsorbed and inserted protein both have circular footprints.
§An approximate expression for $s(m)$ when $m > 4$.

where k is Boltzmann's constant and T is the temperature in degrees Kelvin. The various constants in Eqs. 10 and 12 are given in terms of the footprint areas and circumferences of the three species for both the general case and specific cases in Tables 1 and 2. The constant, Γ, is the edge tension of the lipid bilayer, and D_I is the circumference of the pore, which depends on the number of single ligands, m, making up the pore or aggregate. An expression for D_I is given in Table 1. The factor of two is included because there are two lipid monolayers per bilayer. We can also write the factor, ΓD_I, as follows:

$$\Gamma D_I = \gamma s(m), \tag{13}$$

where γ is given by (using Table 1)

$$\gamma = 2\pi r\Gamma. \tag{14}$$

Here, r is the radius of one of the ligands comprising the pore or aggregate, and $s(m)$ is given in Table 1 for both aggregates and pores. γ has the units of energy and represents the total edge tension for a single ligand (or monomer in the case of pore formation). This quantity, γ, will be used in fitting the theory to specific experimental isotherms for the various ligands or pores. It should be remembered that γ, as defined by Eq. 14, depends on both the nature of the inserted ligand–lipid interface and the spatial dimensions of the ligand itself. Below we will give values for γ in terms of kT for each ligand examined. Dan and Safran (1998) have shown that the edge tension is strongly dependent on the elastic properties of the bilayer (e.g., spontaneous curvature, bending modulus) and the spatial configuration of the inserted ligands. Furthermore, bilayers containing bilayer-forming lipids favor cylindrically shaped ligands, whereas nonbilayer-forming lipids favor shapes that match the spontaneous curvature of the bilayer. The edge tension can have either a positive or negative sign depending on whether insertion is opposed or favored by the bilayer lipids.

The argument of the exponential on the right-hand side of Eq. 10 is directly proportional to the lateral pressure of the adsorbed ligands, and the argument of the exponential on the right-hand side of Eq. 12 is directly proportional to the lateral pressure of the inserted ligands. It is clear from the form of these arguments that these lateral pressures depend on the concentrations of both the adsorbed and inserted ligands. Furthermore, the special case for the insertion of single ligands without pore formation is obtained if the number of ligands, m, is taken as unity and D_I becomes the circumference of the inserted ligand. K_0 is mostly taken as a constant. However, if the equilibrium constant, K_0, is mainly of electrostatic origin, it depends on the ionic strength of the solution and the degree of coverage of the interface (Heimburg and Marsh, 1995; Heimburg et al., 1999). This special case will also be examined explicitly in the next section.

RESULTS

In this section, we present calculations of the isotherms describing the competition between adsorption and insertion of proteins in lipid bilayers using the formalism presented in the previous section with realistic values of the parameters and examine relevant experimental isotherms. As stated above, Chatelier and Minton (1996) have shown that the scaled-particle approach may also be used to describe binding of asymmetric ligands to a surface. Insertion of these

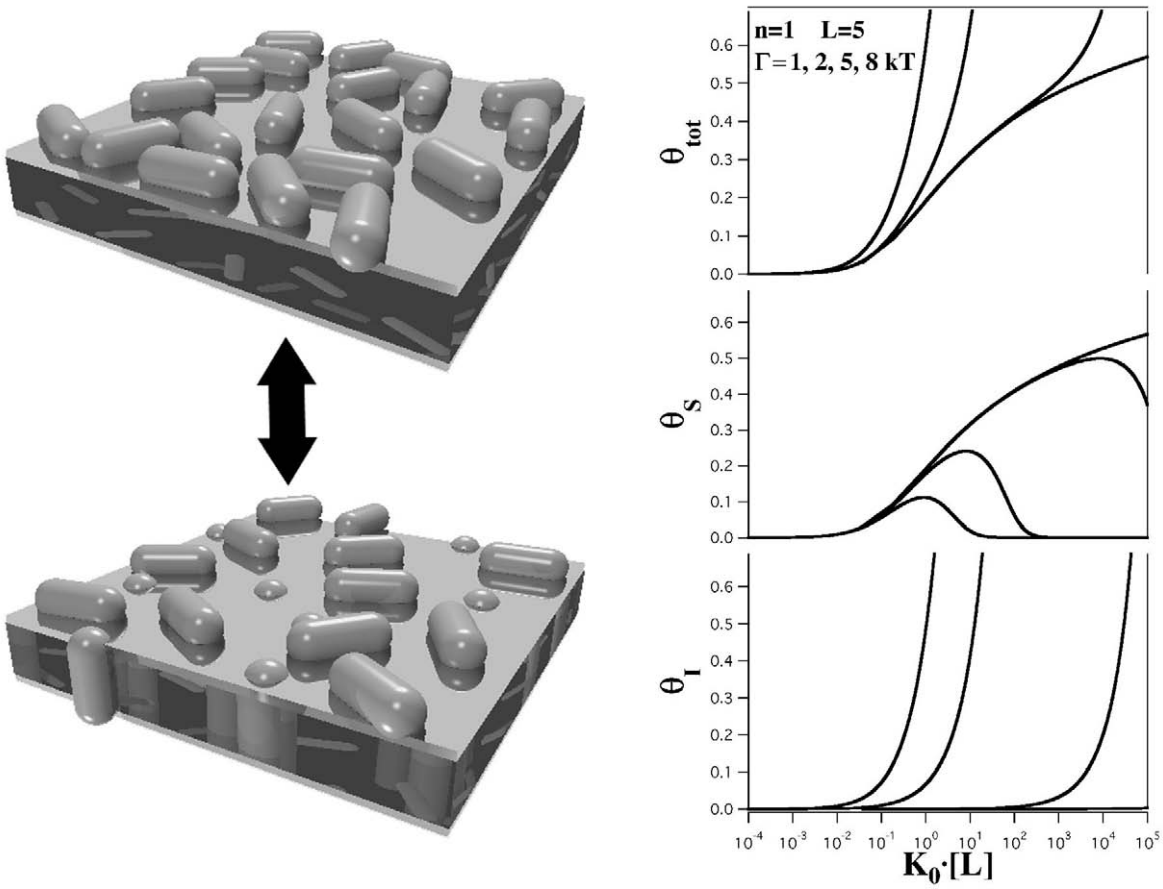

FIGURE 2 *Left*: Insertion scheme for an asymmetric ligand with $L = 5$. *Right*: Binding isotherms for adsorption of this ligand to interfaces and subsequent insertion. *Top panel*, isotherms for the total protein, *center panel*, the interfacially adsorbed species; and *bottom panel*, the inserted fraction, as a function of the free ligand concentration $[L]$ for different values of the edge tension per ligand, $\gamma = 1$, 2, 5, and 8 kT.

ligands into the lipid bilayer results in increasing the surface coverage, which leads to a reduction in configurational entropy that is much more pronounced for asymmetric than for symmetric ligands. As also discussed above, the ability of such ligands to integrate into the bilayer depends directly on the free energy between the ligand and the hydrophobic core of the lipid membranes due to the corresponding edge tension. Naturally, the value of this term is different for different ligands. In our calculations, it is positive when the interfacial adsorption is preferred over insertion and negative in the opposite case. However, at increasing degrees of binding, the free energy of the surface gas formed by the adsorbed ligands at the interface may become large enough to provide the free energy necessary to overcome the barrier for insertion in the case of a positive edge tension. Furthermore, protein insertion changes the overall area of the membrane and thus affects the binding properties.

Such a binding scheme is shown in Fig. 2 (*left*). An asymmetric cylindrical ligand with a ratio of length to diameter of $L = 5$ is allowed to insert such that it spans the membrane perpendicularly. For this insertion, it is affected by an edge tension per monomer of γ per single ligand. The corresponding binding isotherms, based on the numerical solution of Eqs. 9–12 are given in Fig. 2 (*right*). In this figure, the fractional coverage of the lipid bilayer–water interface, θ_S, defined in Eq. 8 (*center panel*), the fractional insertion, θ_I also defined in Eq. 8 (*bottom panel*), and the total bound protein fraction, $\theta_{tot} = \theta_S + \theta_I$ (*top panel*), are shown. The definition of θ_S constrains θ_S to be less than unity, whereas θ_I may become larger than unity because an inserted protein does not occupy membrane area but rather increases the overall area. Isotherms are given for different values of the edge tension, γ, per single ligand defined in Eq. 14 of an inserted ligand. Naturally, at large values of γ, no insertion takes place and proteins bind exclusively to the lipid bilayer–water interface. For low values of γ in the range of $\gamma = 1$–$5kT$, one observes a binding behavior that, upon increase of the free ligand concentration $[L]$, is described by adsorption to the lipid bilayer–water interface followed by an insertion process. Because inserted proteins serve as obstacles for the interfacially adsorbed species, increasing insertion reduces interfacial adsorption and finally leads to its inhibition (Fig. 2, *right*). With respect to the values of γ used in the above calculations, Dan and

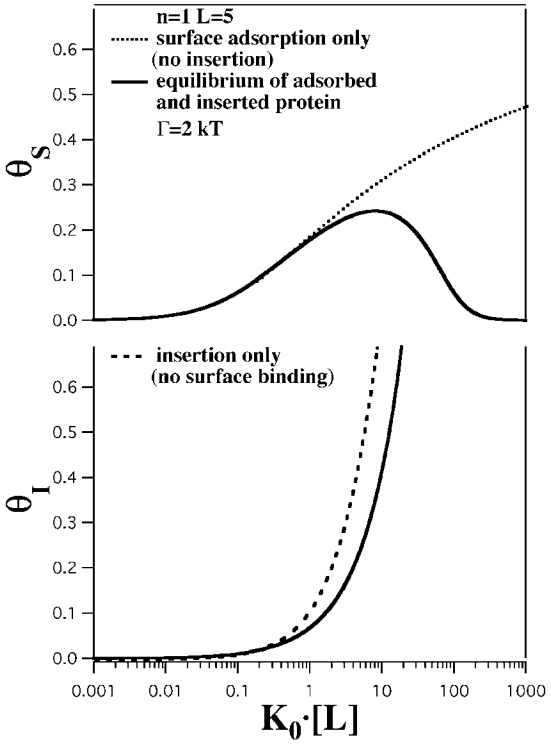

FIGURE 3 The equilibrium of interfacial adsorption and insertion (*solid lines*) leads to isotherms that differ from interfacial adsorption in the absence of insertion (*top panel*, *dotted line*) and from exclusive insertion in the absence of interfacial adsorption (*bottom panel*, *dashed line*). The solid lines represent the equilibrium for $m = 1$, $L = 5$, and $\gamma = 2kT$, taken from Fig. 2. Interfacial adsorption tends to reduce insertion, and vice versa. The effect largely depends on the free ligand concentration $[L]$.

Safran (1998) predict they should lie between 1 and $100kT$ depending on the circumference of the ligand.

The consequences of the competition between adsorbed and inserted species for the available area are examined in Fig. 3 for the case of $\gamma = 2kT$ and $L = 5$ (*solid lines*). This figure shows a continuous increase in the adsorbed species with increasing free ligand concentration, $[L]$ (*dotted line*, *top panel*), for a ligand that cannot insert (e.g., because γ is large and positive). This is equivalent to the results of Minton (1999). Another limiting case is given by a ligand that cannot adsorb onto the lipid bilayer–water interface but can readily insert into the lipid bilayer because it has a low binding affinity to the surface. In this case, $\theta_S = 0$, and Eqs. 11 and 12 give the isotherm,

$$\theta_I = a_B(K_0[L])^m \exp\left(-\frac{2\gamma s(m)}{kT}\right) \times \exp\left[-\frac{a_I'\theta_I}{a_B} - \left(\frac{c_I\theta_I}{a_B}\right)^2\right]. \quad (15)$$

The numerical solution of this equation is given by the dotted line in the bottom panel of Fig. 3 for $m = 1$. Eq. 15 reduces to the linear equation for partitioning of ligands between the aqueous medium, and the lipid bilayer as given by classical solution theory (mass action) when the exponential term on the right-hand side is replaced by unity. Because the exponent of this exponential term is directly proportional to the lateral pressure exerted on the membrane by the inserted ligand, Eq. 15 can be thought of as a Gibbs isotherm for partitioning. The isotherms shown as dotted lines in Fig. 3 change when both adsorption and insertion of the ligands can occur, as shown by the solid lines in Fig. 3 for each case.

Figure 3 shows in particular that, for positive edge tensions, insertion occurs at a higher free ligand concentration than in the absence of interfacial adsorption. If the adsorbed and inserted species coexist at positive values for γ, the ligands will always prefer adsorption up to a threshold value where the chemical potential of the adsorbed species overcomes the edge tension necessary for insertion. At high degrees of insertion, the adsorption onto the interface is inhibited.

This situation is even more pronounced when the inserted ligands form aggregates of m monomers, as is likely to be the case for the association of melittin (Ladokhin et al., 1997) or gramicidin S (A. Ulrich, Jena, private communication) with lipid bilayers. First, insertion is more cooperative because m interfacially adsorbed monomers insert simultaneously to form an m-mer. Second, the m-mer is less of an obstacle to the adsorbed ligand. Third, the distributional entropy of the inserted m-mer is lower than that of m separately inserted monomers. In Fig. 4 (*left*), we schematically describe a situation where the m-mer forms a circular pore. The data in Fig. 4 (*right*) is presented in the same manner as that of Fig. 2. In the right-hand panel of Fig. 4, the adsorption and insertion isotherms are given as functions of the free ligand concentration for the insertion of a 6-mer ($L = 5$) and several values for γ. The interface between inserted protein and the lipid bilayer now consists of the outer surface of the pore-forming 6-mer. Upon a sudden decrease in interfacial adsorption, insertion occurs much more abruptly as compared to the insertion of monomers. Thus, complete insertion occurs over a very narrow interval of the free ligand concentration. Subtle changes in the range of 10% of the free ligand concentration may reversibly induce insertion. This provides a putative control over insertion processes.

Our concept is based on the competition between interfacially adsorbed and inserted proteins for available area at the interface. This competition is strongly affected by the lateral pressure of the surface gas formed by the bound ligands, which is solely built up by hard core repulsion (excluded volume). To examine the competition in more detail, we now consider the binding of two ligand species, A and B, to a lipid bilayer where species A, unlike species B, is allowed to insert into the membrane. However, upon adsorption, species B still occupies interfacial area and thus

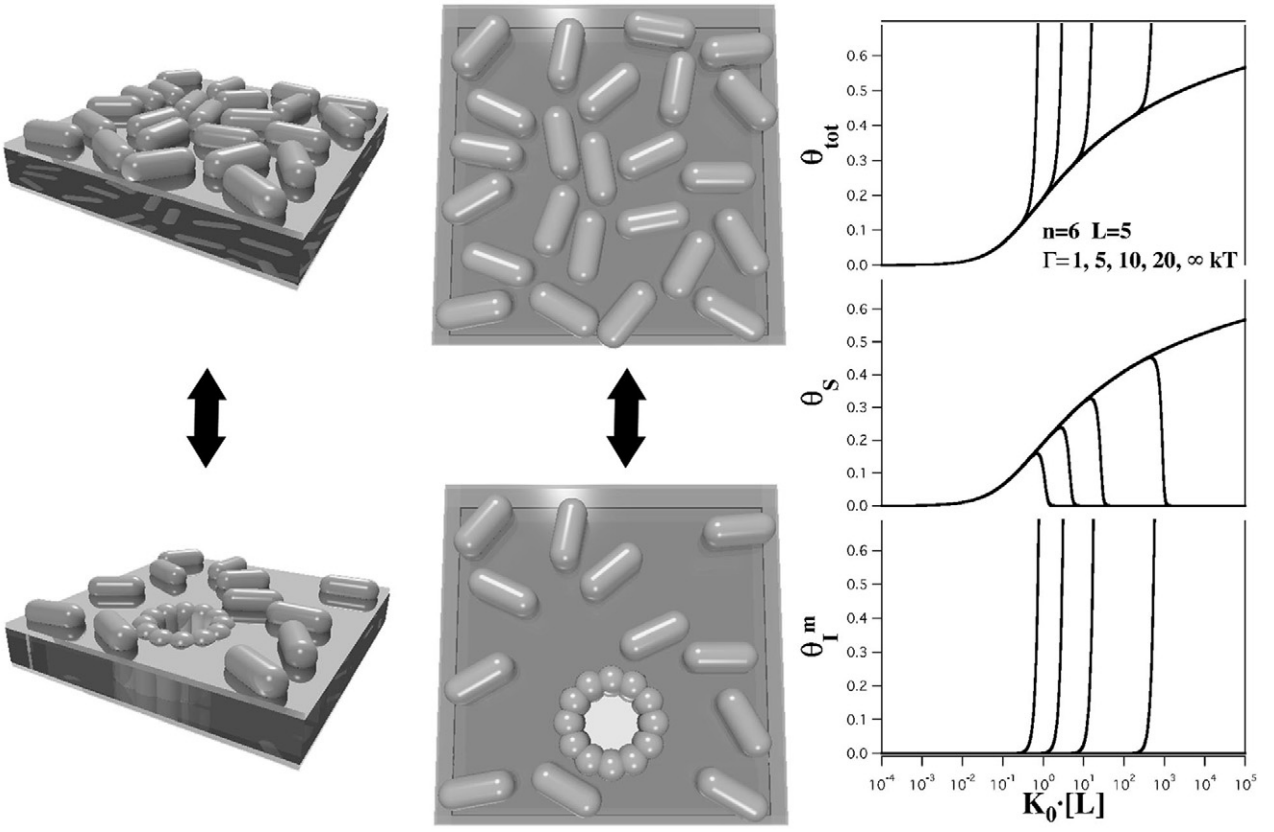

FIGURE 4 *Left* and *center*: Insertion scheme for an asymmetric ligand with $L = 5$ that forms pore-like aggregates of size m. *Right*: Binding isotherms for adsorption of this ligand to the interface and subsequent insertion as pore-forming aggregates of size $m = 6$. *Top panel*, isotherms for the total protein; *center panel*, the interfacially adsorbed species and *bottom panel* the inserted fraction, as a function of the free ligand concentration for different values of the edge tension per ligand $\gamma = 1$, 5, 10, 20, and $30kT$. Insertion is favored as compared to nonaggregating proteins (Fig. 2). The equilibrium between adsorbed and inserted protein depends more sensitively on the free ligand concentration $[L]$.

influences the lateral pressure of the surface gas and therefore the chemical potential of species A. Figure 5 (*left*) shows that the adsorption of species B (*dark cylinders*) has a considerable effect on the adsorption–insertion equilibrium of species A (*light cylinders*).

In Fig. 5 (*right*), we show the effect of changing the free concentration of species B on adsorption and insertion of species A. In the calculations, we varied $K_{A,0}[L_A]$ but keep $K_{B,0}[L_B]$ constant. The isotherms for three different values of $K_{B,0}[L_B]$, 0, 1, and 100, exhibited in Fig. 5, show that the adsorption of ligand B has only a slight effect on the adsorption/insertion equilibrium of ligand A. Although insertion of ligand A is slightly reduced as the concentration of ligand B is increased, the degree of adsorption of ligand A is substantially reduced, indicating that the two ligands compete for available space on the lipid bilayer–water interface.

Adsorption of ligands in the absence of dissociation

We have so far restricted our formalism to the case of ligands that bind to the lipid bilayer and dissociate from it under equilibrium conditions. In the case of highly hydrophobic ligands such as melittin or alamethicin, it is reasonable to assume that they only adsorb but do not dissociate, in which case the effect of ligand competition on protein insertion will be different from that depicted in Fig. 5. This is, of course, an idealization of a realistic case, where some dissociation occurs (Kessel et al., 2000, reported relatively low free energies for dissociation of alamethicin). To model this situation, we consider the case of two ligands, A and B, of similar shape, each of which has a fixed value of the total fraction density, $\theta_T^\alpha(\alpha = \text{A, B})$ in the lipid bilayer. Furthermore, each ligand may either lie on the interface or insert into the lipid bilayer as a component of an m-mer pore. Under these conditions, the binding is described by

$$\theta_I^\alpha = (a_B - a_S\overline{\theta_S}^{(1-m)}[a_S\theta_S^\alpha]^m \exp(-\kappa^\alpha(\overline{\theta_S}, \overline{\theta_I})), \quad (16)$$

$$\alpha = \text{A, B}, \quad \theta_T^\alpha = \theta_S^\alpha + m\theta_I^\alpha$$

$$\overline{\theta_S} = \theta_S^A + \theta_S^B, \quad \overline{\theta_I} = \theta_I^A + \theta_I^B,$$

where θ_S^α and θ_I^α are the concentrations of the adsorbed

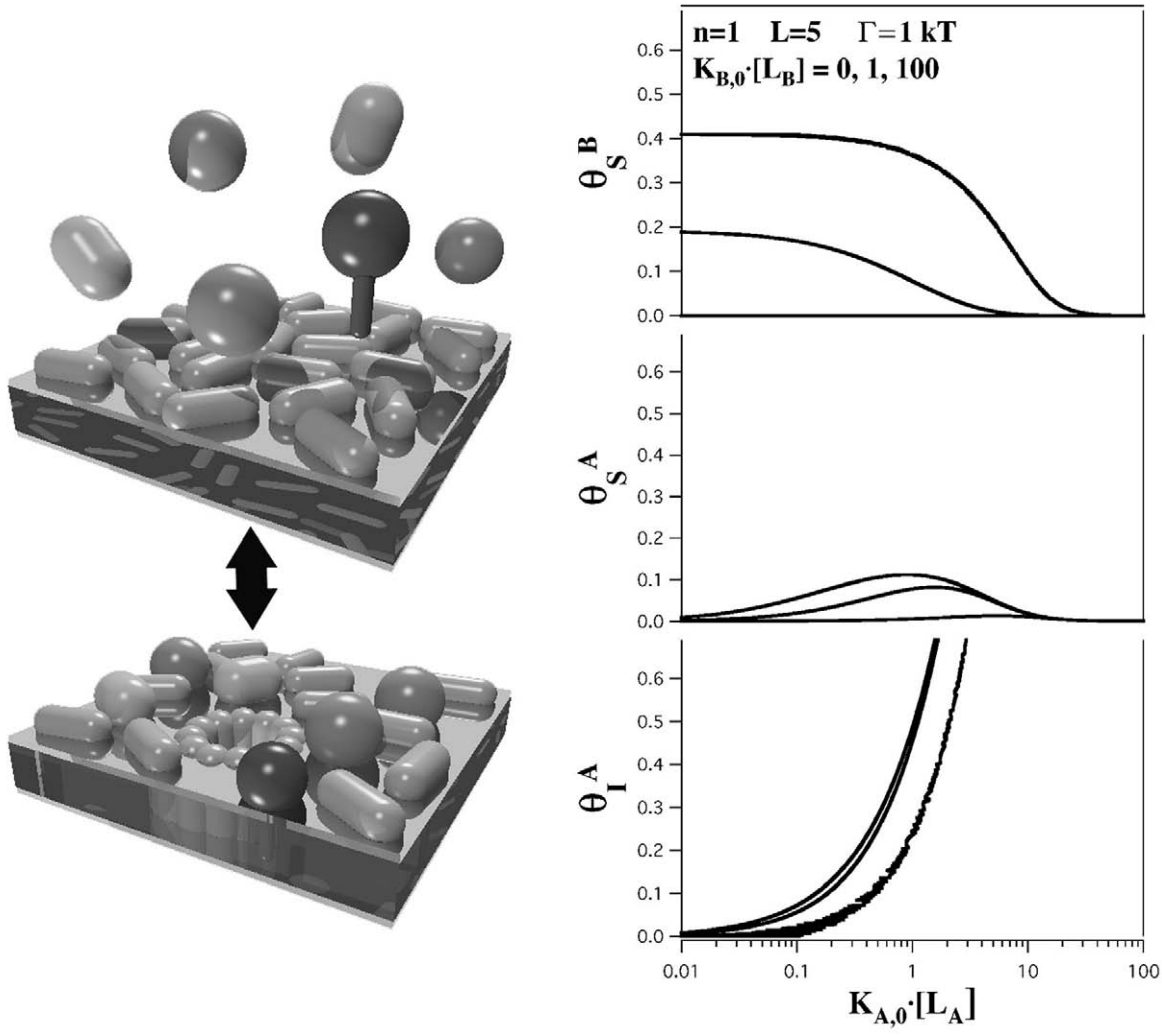

FIGURE 5 *Left*: Insertion scheme for an asymmetric ligand with $L = 5$ (*light cylinders*) that forms pore-like aggregates of size m in the presence of a second protein species that can only adsorb to the interface (*black cylinders*). *Right*: Binding isotherms for adsorption of this ligand to interfaces and subsequent insertion as pore-forming aggregates of size $m = 6$ in the presence of a second adsorbing species that cannot insert. *Top panel*, isotherms for species B; *center panel*, the interfacially adsorbed species A; and the *bottom panel* inserted fraction of species A, as a function of the free ligand concentration of species A for an edge tension $\gamma^{(\alpha)} = 5kT$. The various curves in each panel correspond to different values of the free ligand concentration, L_B ($K_{0,B} \cdot [L_B] = 0, 1, 200$).

ligands and inserted pores, respectively, of species α and the function, $\kappa(\overline{\theta_S}, \overline{\theta_I})$, is given by

$$\kappa^{\alpha}(\overline{\theta_S}, \overline{\theta_I}) = \left(\frac{2\gamma^{\alpha}s(m)}{kT}\right)\left(\frac{a'_S\overline{\theta_S} + a'_{SI}\overline{\theta_I}}{a_B - a_S\overline{\theta_S}}\right) + \left(\frac{b_S\overline{\theta_S} + b_I\overline{\theta_I}}{a_B - a_S\overline{\theta_S}}\right)^2 - m\left[\frac{a''_{SI}\overline{\theta_S} + a'_I\overline{\theta_I}}{a_B - a_S\overline{\theta_S}} + \left(\frac{c_S\overline{\theta_S} + c_I\overline{\theta_I}}{a_B - a_S\overline{\theta_S}}\right)^2\right], \quad (17)$$

where $\gamma^{(\alpha)}$ is the edge tension per ligand for species α. Here we have assumed, for simplicity, that the spatial dimensions of the adsorbed species and pores are the same for both species. Note that each species can both adsorb and insert.

Using this set of equations in conjunction with the parameters defined in Table 2, we calculated the adsorption/insertion equilibrium of ligand A as a function of the total concentration of ligand B. The left-hand panel of Fig. 6 shows the case when ligand B is located solely in the lipid bilayer–water interface (no insertion, $\gamma \to +\infty$) and the right-hand panel shows the case when ligand B is only inserted ($\gamma \to -\infty$). It can be seen from this figure that the insertion of ligand A is strongly promoted by increasing the concentration of ligand B, although the effect is different in each case. In contrast, the effect of adsorbing of a second species of ligand was different for the situation described in Fig. 5 because the second species in this case could preferably dissociate from the lipid bilayer once the concentration of inserted ligands of the first species exhibited a considerable increase.

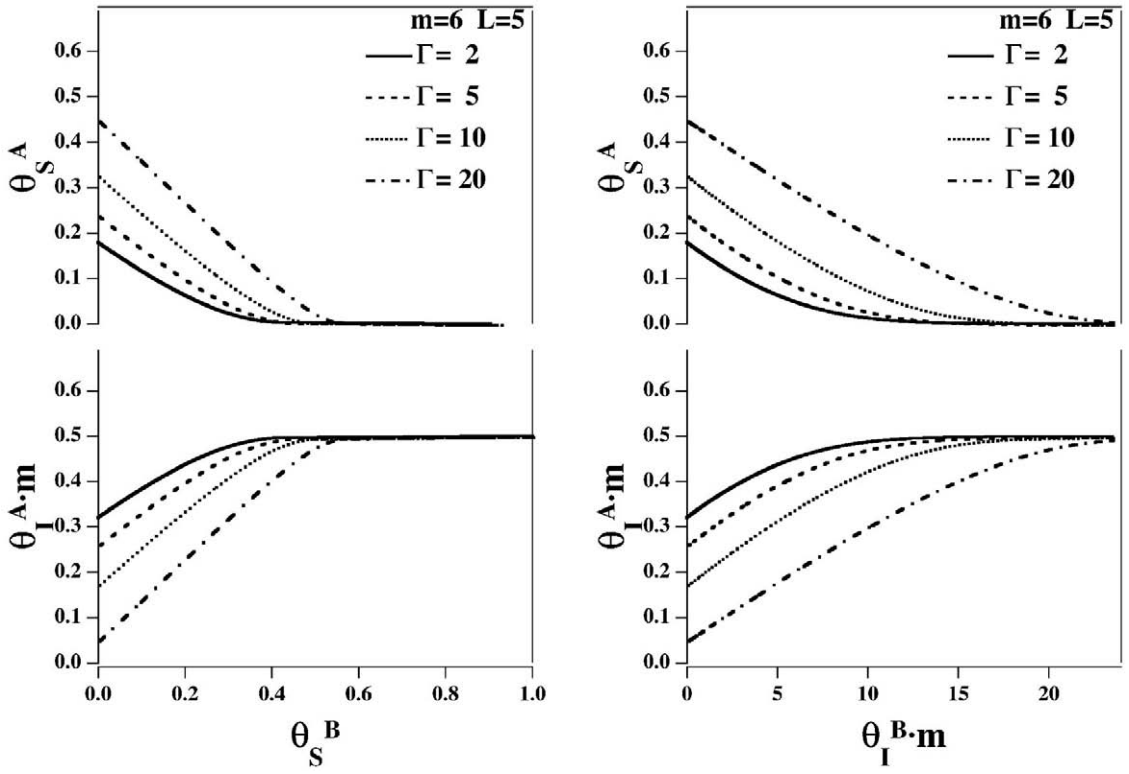

FIGURE 6 Equilibrium of adsorbed and inserted protein of species A with constant concentration $\theta_S^{(\alpha)} + \theta_I^{(\alpha)} = 0.5$ as a function of the concentration of a second ligand, B. Conditions are chosen such that both ligands cannot dissociate or desorb from the membrane. Both ligands have identical shapes. *Left*: B only binds to the interface. *Right*: B only inserts into the bilayer. Parameters are $m_{A,B} = 6$ and $\gamma_1 = 2$, 5, 10, and 20kT.

Binding of cytochrome *c* to lipid bilayers

We used the present approach to analyze the binding of the mitochondrial protein cytochrome *c* to DOPG lipid bilayers. It had previously been proposed that cytochrome *c* inserts into the bilayer at low ionic strength. DOPG has one net negative charge, whereas cytochrome *c* has an effective positive charge of ~4 and the binding affinity is of electrostatic origin. This results in a dependence of the intrinsic binding constant, K_0, on the ionic strength and the degree of interfacial coverage. Heimburg and Marsh (1995) derived the following expression for the interfacial charge density of a lipid bilayer with proteins adsorbed to the lipid bilayer–water interface,

$$\sigma = \left(1 - \frac{Z}{\alpha}\theta_S\right)\frac{e}{f_0}, \tag{18}$$

where Ze is the effective positive charge of the protein, and α is the number of lipid molecules of area f_0 with one net negative charge in a binding site. This results in an expression for the intrinsic binding constant, K_0,

$$K_0 = 0.5\alpha[\mathrm{Na}^+]\left(1 - \frac{Z}{\alpha}\theta_S\right)^{-2Z}, \tag{19}$$

where $[\mathrm{Na}^+]$ is the free sodium concentration. In this formalism, the charge density of the lipid–protein complexes is approximated by a smeared out, homogeneous value that is equivalent to a mean field approximation. Using a similar model as described in this paper, Heimburg et al. (1999) obtained a lipid/protein stoichiometry of $\alpha = 7.8$ by fitting to the experimentally determined isotherms and an effective charge $Z = +3.8$ of cytochrome *c*, which was deduced from the ionic strength dependence of the intrinsic binding constant. Cytochrome *c* is almost perfectly spherical with a diameter of 30 Å. It was found that the binding of this protein to charged lipid bilayers could be explained by the interfacial absorption of hard spheres, provided that the monovalent salt concentration is higher than 40 mM. The isotherms for interfacial adsorption under these conditions are well described by

$$K_0[L] = 0.5\alpha[\mathrm{Na}^+]\left(1 - \frac{Z}{\alpha}\theta_S\right)^{-2Z} \times \frac{\theta}{1-\theta}\exp\left(\frac{3\theta}{1-\theta} + \left(\frac{\theta}{1-\theta}\right)^2\right). \tag{20}$$

This equation can be derived from Eqs. 2 and 19.

The experimental data of Heimburg and Marsh (1995) and the calculated isotherms are given in Fig. 7 *a* (*left panel*). These data show that, below a threshold of 40 mM NaCl, the binding capacity of the membrane is considerably increased such that more protein binds than can be ex-

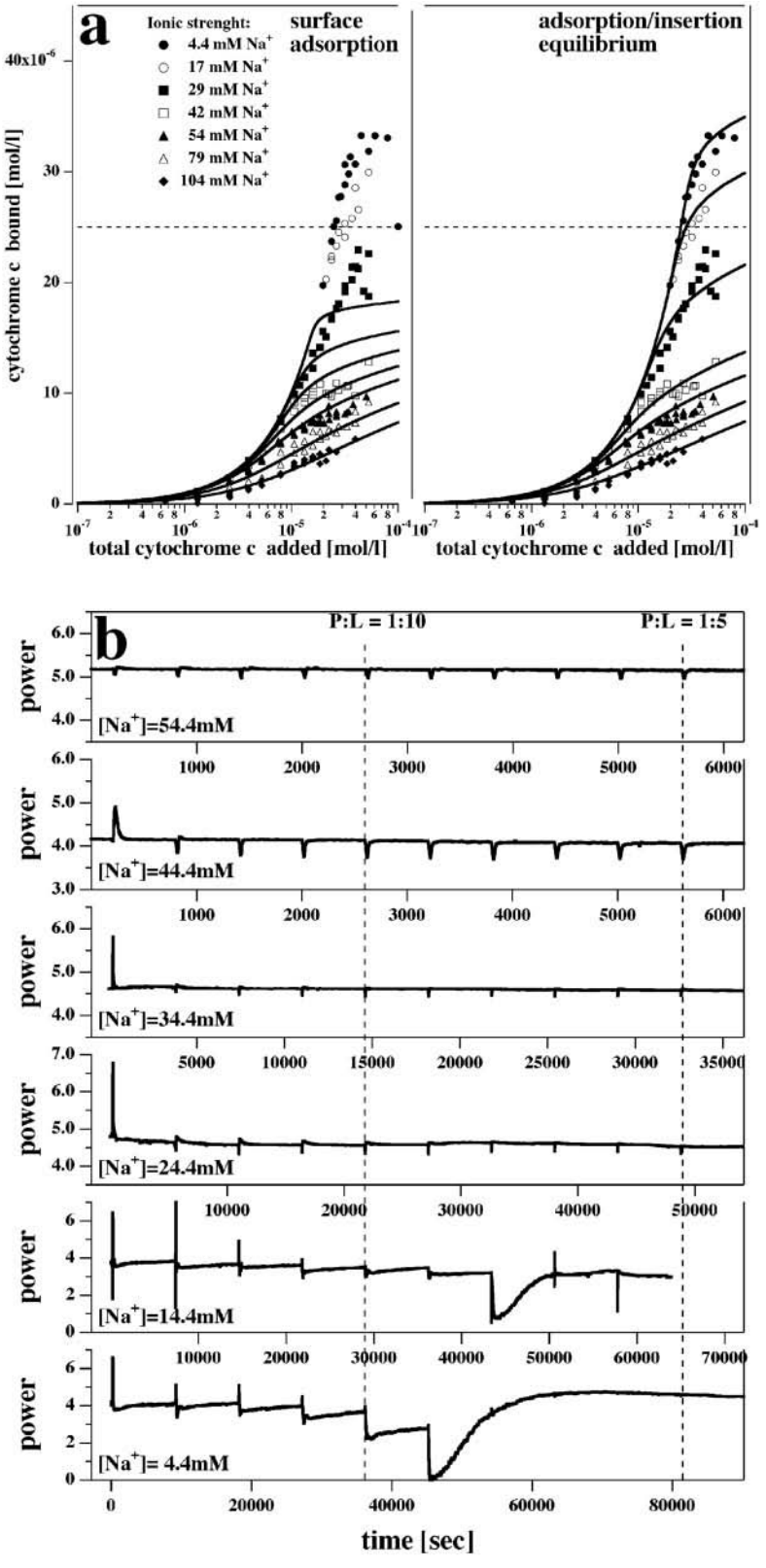

FIGURE 7 (*a*) Binding of cytochrome *c* to DOPG bilayers as a function of the total cytochrome *c* concentration obtained at different ionic strengths. The symbols denote experimental data as adapted from Heimburg and Marsh (1995). The solid lines represent the calculated isotherms. *Left-hand panel*: It was assumed that no insertion takes place. The intrinsic binding constant, K_0, was modified such that electrostatics is taken into account (see Eq. 19). At sodium chloride concentrations above 40 mM, the isotherms are well described by pure interfacial adsorption. At lower ionic strengths, the binding capacity of the lipid bilayers for cytochrome *c* is much larger than predicted for interfacial adsorption alone. The figure shows explicitly that it actually exceeds the maximum binding capacity of the interface (*horizontal dashed line*). *Right hand panel*: The calculated isotherms for an adsorption/insertion equilibrium. The intrinsic binding constants are now given by Eqs. 21 and 22. It was assumed that the protein may insert as a monomer with a positive edge tension per monomer of 8-*kT* for $c > 50$ mM, 7*kT* for $c = 42$ mM, and 5-*kT* for $c = 4-40$ mM. This indicates that insertion of cytochrome *c* is unfavorable. (*b*) Titration calorimetric data of cytochrome *c* binding to DOPG membranes at six ionic strengths from 4.4 mM Na^+ to 54 mM Na^+ concentration. At 54 mM Na^+, no insertion is predicted, whereas, at 4 mM Na^+, insertion is assumed from the fits of panel (*a*). The binding modes at the two ionic strength conditions are very different, supporting the above assumption. At 4.4 mM Na^+ and 14.4 mM Na^+, a fast process is followed by a very slow process with strong heat absorption, which becomes dominant at high degrees of binding, which are above full surface coverage. At 54 mM Na^+, however, binding is a simple, fast process with very small heat. The units of the power axes are [μcal/sec]. Note the different scaling of time and power axes for the different experiments.

plained by the available area on the lipid bilayer–water interface. This implies that Eq. 20 considerably underestimates the binding capacity of the lipid bilayer at low ionic strength (see solid lines in Fig. 7 *a*, *left*). Figure 7 *a* clearly shows that the binding data of Heimburg and Marsh for cytochrome *c* cannot be interpreted qualitatively in terms of

the theory for single-layer adsorption when the ionic strength is low and the intrinsic binding constant is high. In addition, Heimburg and Marsh (1995) found that, under these conditions, their data from ESR experiments could be interpreted in terms of a distortion of the hydrophobic core of the lipid bilayer. This led to the conclusion that, at low ionic strength (high intrinsic binding constant) and high degrees of interfacial occupancy, cytochrome *c* inserts into the hydrophobic core of the membrane rather than adsorbing in more than one layer on the lipid bilayer–water interface.

If insertion into the bilayer occurs, there are different electrostatic contributions for inserted and adsorbed proteins, because inserted proteins increase the overall area of the bilayer and thus reduce the charge density. Using the formalism of Heimburg and Marsh (1995), the binding constants for the adsorbed species are given by

$$K_S^{el}(\theta_S, \theta_l) = 0.5\alpha[Na^+] \cdot \left(1 - \frac{(\theta_S + \theta_i)\,(Z/\alpha)}{(1 + \theta_i)}\right)^{2Z}, \quad (21)$$

and, for the inserting species, is given by

$$K_I^{el}(\theta_S, \theta_l) = 0.5\alpha[Na^+] \cdot \left(1 - \frac{(\theta_S + \theta_l)(Z/\alpha)}{(1 + \theta_l)}\right)^{2Z} \cdot \exp\left(2\alpha\left[\frac{1 - (\theta_S + \theta_l)(Z/\alpha)}{(1 + \theta_l)}\right]\right) \cdot e^{2\alpha}. \quad (22)$$

These terms take into account the dependence of the electrostatics on the ionic strength and on the charge density of the membrane. The two new binding constants replace the intrinsic binding constants, K_0 and K_0^m, in Eqs. 10 and 12, respectively.

We were, in fact, able to fit the binding data of Heimburg and Marsh (1995) in a reasonable manner using the analysis for adsorption/insertion equilibrium described in the Theory section in conjunction with Eqs. 21 and 22. These fits are given in Fig. 7 *a* (*right panel*). We assumed that the conformation of cytochrome *c* is unchanged upon insertion and that cytochrome *c* inserts as a monomer. It was found that the edge tension per monomer assumed values between $\gamma = 5kT$ and $\gamma = 8kT$ suggesting that insertion is unfavorable but can occur at high degrees of surface coverage of protein.

Titration calorimetry

To investigate the binding of cytochrome *c* to DOPG membranes in more detail, we performed titration calorimetry experiments, and the data is shown in Fig. 7 *b*. The experimental details are given in Materials and Methods. Because fitting the isotherms shown in Fig. 7 *a* implied that the protein inserts in the ionic strength regime between zero and 30 mM Na^+, we studied the calorimetric isotherms in the range of 4–54 mM Na^+ (see Fig. 7 *b*). In this experiment, we injected 10 μl of a 1.61-mM cytochrome *c* solution into a 0.536 mM DOPG dispersion, after which the heats of reaction were recorded. The binding reaction changed quite dramatically over the six different salt concentrations chosen, but was often extremely slow. Therefore, the time interval between two injections was, in some cases, chosen to be as high as 2.5 h. Figure 7 *b* clearly shows that, at 4-mM Na^+ and 14-mM Na^+, the titration isotherm is biphasic, exhibiting a fast reaction followed by a very slow process, which is highly endothermal (note the different scaling of time and power axes for the various experiments in Fig. 7 *b*). A second mode of interaction is thus observed under conditions where insertion is expected. Heats of binding are very small at higher salt concentration. We suggest that the slow endothermal reaction, which is shown in the last two titration experiments (Fig. 7 *b*), can be associated with the insertion process. A similar biphasic binding reaction has previously been observed by Heimburg and Biltonen (1994) for the case of cytochrome *c* binding to dimyristoyl phosphatidylglycerol. In this paper, insertion was not considered. However, it was concluded that, there, cooperative changes in the lipid/protein complex occur at high protein concentrations.

Binding of endotoxin to lipid bilayers

δ-Endotoxins are highly potent pore-forming insecticidal toxins produced by *Bacillus thuringiensis* (Gazit et al., 1998). Each toxin consists of three domains: domain I is the pore-forming domain consisting of six α-helices surrounding the central α5-helix; domain II is rich in β-sheets and binds to a membrane receptor; and domain III consists of two β-sheet sandwiches. Gazit et al. (1998) studied the binding of the α-helical fragments of domain I to zwitterionic model membranes and found a cooperative binding behavior for the α5-helix, which is shown in Fig. 8 *a*. The related binding mechanism postulated by Gazit et al. (1998) and Shai (1999) consists of a peptide adsorption step followed by insertion of the peptide into the membrane. This is the exact process described theoretically by our model. Figure 8 *a* contains a fit to the experimental isotherm for the α5-helix using Eqs. 9 and 11. To compare our calculations with the experimental data, we assumed that the endotoxin helix is ~1 nm in diameter and 3.45 nm in length (23 amino acids). Thus the shape parameter L is equal to 3.45. Assuming an area of 0.5 nm^2 per lipid molecule, each interfacially adsorbed peptide covers about seven lipids. These values have been used to convert the fraction of bound peptide given in the paper by Gazit et al. (1998) into a fractional surface coverage θ, as used in our formalism (cf., the ratio between right- and left-hand axis scaling in Fig. 8). As shown in Fig. 8 *a*, we are able to make a remarkably good fit to the experimental isotherms using a value of $\gamma = -10.5kT$ for the edge tension per monomer and a pore size of $n = 9$ peptides. Although the edge tension of the inserting peptide is negative, indicating a favorable insertion, it is

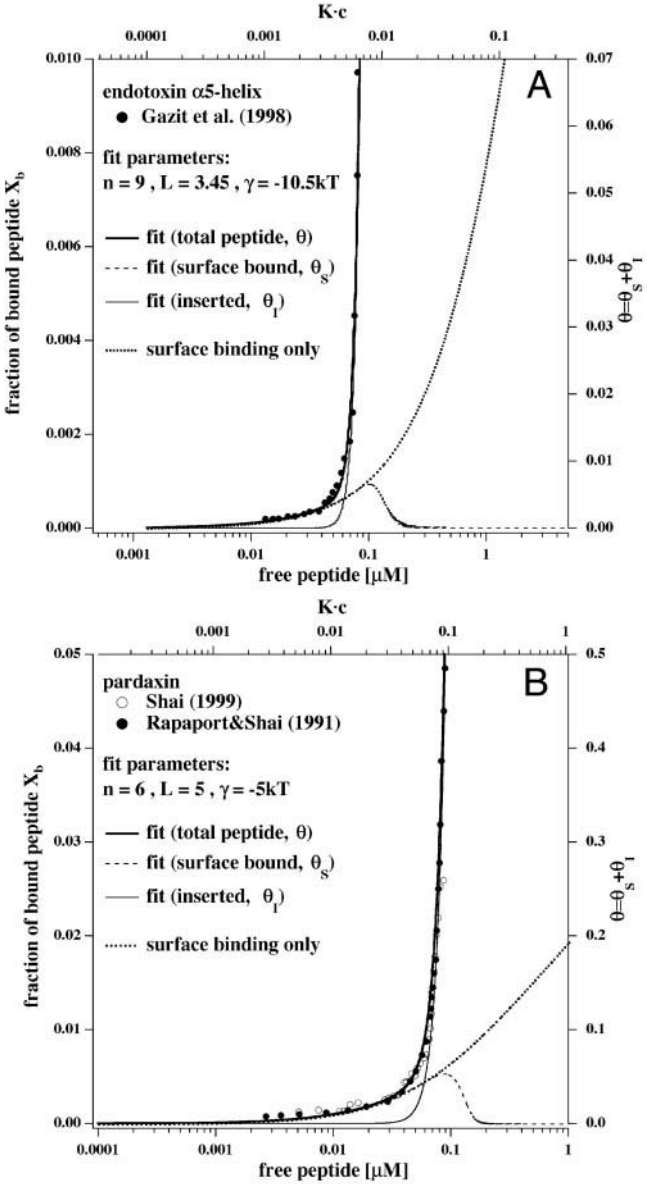

FIGURE 8 (*A*) Adsorption and insertion of the pore-forming endotoxin α5-helix into phosphatidylcholine membranes (data taken from Gazit et al. (1998)). The fit takes into account the physical size of the helices, using a pore size of $n = 9$ and an edge tension per monomer of $\gamma = -10.5$, indicating a favorable insertion. Both the interfacially adsorbed and the inserted fractions are shown. As a comparison, the isotherm for pure interfacial adsorption is also given. In the analytical procedure, it was assumed that the physical origin of the binding process is not electrostatic in nature because the lipids are zwitterionic. (*B*) Adsorption and insertion of the pore-forming pardaxin peptide (33 amino acids into phosphatidylcholine membranes (Data taken from Rapaport et al. (1991) and Shai (1999). The fit takes into account the physical size of the helices, using a pore size of $n = 9$ and an edge tension per monomer of $\gamma = -5kT$, indicating a favorable insertion. Both the interfacially adsorbed and the inserted fractions are shown. As a comparison, the isotherm for pure interfacial adsorption is also given. As for endotoxin, it was assumed that the physical origin of the binding process is not electrostatic in nature.

shown in Fig. 8 *a* that, at low endotoxin α5-helix concentrations, most of the peptide adsorbs to the surface.

Binding of pardaxin to lipid bilayers

Pardaxin is a neurotoxic peptide with 33 amino acids and is a main component in the secretion of the Red Sea Moses sole fish where it acts as shark repellent. Rapaport and Shai (1991) and Shai (1999) investigated the binding of various mutants of this peptide to zwitterionic model membranes. These authors report that pardaxin displays a cooperative binding isotherm similar to that of the endotoxin α5-helix. We modeled the binding behavior by assuming that the pardaxin helix is ~1 nm in diameter and 5 nm in length (33 amino acids). The shape parameter L is thus equal to 5. Assuming an area of 0.5 nm^2 per lipid molecule, each surface-adsorbed peptide covers ~10 lipids. These values have been used to convert the fraction of bound peptide given in the paper by Rapaport and Shai (1991) and Shai (1999) to a fractional surface coverage θ as used in our equations. The experimental data for paradaxin and a pardaxin mutant are given in Fig. 8 *b* and are well described by our insertion model, assuming an edge tension per monomer of $\gamma = -5kT$ and a pore size of $n = 6$. The binding characteristics compare well with the analogous behavior of the endotoxin α5-helix, and the two pore-forming peptides both require negative edge tensions. This is in contrast to our fits to the cytochrome *c* isotherms, which require positive edge tensions. The fits show that insertion of both the endotoxin α5-helix and pardaxin into the lipid bilayer is favored and occurs at low concentrations of peptides, whereas chytochrome *c* insertion is unfavorable and only occurs at very high degrees of surface coverage.

DISCUSSION

In this work, we used the scaled particle formalism of Minton (1999) to derive equations for isotherms related to ligands that can both adsorb onto a planar surface and insert into that surface. Here, the surface represents the interface of a lipid bilayer membrane, and the ligands can be thought of as either peptides or proteins. We considered the following four cases in the theoretical analysis:

1. the adsorption of an asymmetric peptide and its insertion with a perpendicular orientation as shown in Fig. 2;
2. the adsorption of the asymmetric peptide of case 1 and its insertion as a pore-like aggregate formed from six monomers as shown in Fig. 4;
3. case 2 in the presence of a second adsorbed species, again an asymmetric ligand with the same shape as the first species as shown in Fig. 5;
4. two bound ligand species, each with a constant concentration in the lipid bilayer with no possibility of desorption or dissociation from the lipid bilayer.

In case 4, the second species of ligand could either insert or lie on the interface, whereas the first species could be in both locations in the lipid bilayer.

It is important to note that the isotherms themselves are Gibbs rather than Langmuir isotherms with the result that the surface gas formed by the adsorbate and that formed by the inserted ligands (or pores) exert competing lateral pressures on the system. The various species have to overcome these pressures to insert or adsorb. In addition, the ligands (or pores) must, in some cases, overcome a positive edge tension around their boundaries to insert. The results are quite significant and follow the analysis in Fig. 3. As the concentration of the bulk ligand $[L_A]$ increases, the ligands first adsorb onto the planar surface and the concentration of inserted ligands (pores) is negligible. At a certain concentration related to the value of the edge tension, the ligands insert rapidly with $[L_A]$ while the concentration of adsorbed ligands decreases quickly to almost zero. The interval of values of $[L_A]$, where there is appreciable adsorption plus appreciable insertion, is quite small for case 1 and negligible for cases 2 and 3. In fact, for pores composed of six ligands, the processes of adsorption and insertion are almost mutually exclusive.

Next, we examined three applications to experimental data for the binding of ligands to lipid bilayers: cytochrome *c*, the α5-helix of endotoxin (Gazit et al., 1998; Shai, 1999) and pardaxin (Rapaport and Shai, 1991; Shai, 1999). For the case of the binding of cytochrome *c* to DOPG bilayers, the experimentally obtained isotherms could not be interpreted directly in terms of the theory in the second section for pure interfacial adsorption in conjunction with the expression for the binding constant $[K_0]$ of Eq. 19. Because, in addition to this situation, the presence of a distortion of the central membrane core was inferred from ESR experiments, we concluded that, at low ionic strength (i.e., high intrinsic association constant K_0), cytochrome *c* inserts into the lipid bilayer rather than adsorbing onto the lipid bilayer–water interface in more than one layer. Our theoretical analysis of the binding isotherms suggests that the edge tension of the inserted protein is positive, implying that insertion is unfavorable at low concentrations. Note that the expression of Eq. 19 for $[K_0]$ is of electrostatic origin and therefore depends on both adsorbate and inserted concentrations. Now, titration calorimetry is able to distinguish different modes of interaction in the cytochrome *c* experiments, whereas ultracentrifugation assays (Fig. 7 *a*) are unable to do so. Using isothermal titration calorimetry, we found two modes of interaction at the ionic strengths conditions for which insertion is predicted. The first mode is a fast reaction, whereas the second mode is very slow (time scale up to hours) and clearly cooperative.

The prediction that cytochrome *c* inserts into anionic lipid membranes is supported by other experimental results. As mentioned above, ESR experiments suggested that cytochrome *c* interacts with the central core of the bilayer at low ionic strength. At higher ionic strength, no such interaction was found. Furthermore, titration of cytochrome *c* to dipalmitoyl phophatidylglycerol membranes at low protein concentrations leads to a shift of the lipid chain melting transition at ~41°C to higher temperatures as observed using differential scanning calorimetry. Upon increase of the protein concentration, this transition shifts abruptly to lower temperatures with quite different melting profiles (data not shown).

The isotherms for the binding of the two pore-forming peptides, the endotoxin α5-helix and pardaxin, to lipid bilayers were obtained from fluorescence measurements. We found that they are well described by our model when using a negative edge tension per monomer. This implies that, in contrast to cytochrome *c*, insertion of these peptides into lipid bilayers is energetically favorable.

As stated in the Introduction, there is a considerable number of additional examples of reversible insertion and pore formation in lipid bilayers and biomembranes by various species of ligand. These include melittin and magainin (Bechinger, 1999; Ducarme et al., 1998; Ladokhin et al., 1997; Pramanik et al., 2000; Vaz Gomez et al., 1993; Yang et al., 2000), gramicidin S (A. S. Ulrich, personal communication), alamethicin and poly-ene antibiotics (e.g., amphotericin B; Hartsel et al., 1993) and some amphipathic model peptides (Bechinger, 1999). Among these examples, gramicidin S, a cyclic decapeptide, and some highly helical model peptides behave in the manner described in the Results section. The reversible insertion of such peptides can be studied by solid state NMR on oriented bilayers (Bechinger et al., 1996). For example, A. S. Ulrich and coworkers (Salgado et al., 2000) investigated the interaction of fluorinated gramicidin S with oriented pure lipid bilayers using solid state ^{19}F-NMR spectroscopy. They observed adsorption followed by insertion as a function of gramicidin S bulk concentration in the solute by considering the orientation of the peptide. In particular, the change from adsorption to insertion with a concomitant change in orientation was observed directly from the NMR data. An analogous situation is described in a review by Bechinger (1999) for amphipathic model peptides in pure lipid bilayers, where a change in pH rather than in bulk peptide concentration was used as the external variable. In this case, the change in pH can be expected to alter the edge tension of the inserted peptides. The same review contained a description of how melittin reversibly inserts upon increase of melittin concentration. This is in agreement with model simulations by Ducarme et al. (1998), which predict a dynamic equilibrium between interfacially adsorbed and inserted peptides for melittin and, to a certain degree, for magainin. The work by Ladhokin et al. (1997) on the interaction of melittin with POPC vesicles using two sizes of dextrane initially located inside the vesicles shows that inserted melittin does indeed form pores for not too high bulk melittin concentrations at which rupture occurs. Furthermore, these pores increase in

diameter as the bulk melittin concentration is increased. Pore formation of melittin was also found by Ohki et al. (1994) and Pramanik et al. (2000) by analyzing the release of fluorescence labels from vesicle interior. A similar effect was found for magainins. Although many studies report that magainins only adsorb on lipid bilayer–water interfaces of model membranes, they appear to display strong heterocooperativity in biological membranes, and this leads to pore formation of membrane-spanning magainins (Vaz Gomez et al., 1993). These pores then exist in equilibrium with interfacially adsorbed monomers. We plan to examine all these effects by using and extending the formalism of the Theory section.

The authors wish to thank Dr. Terry Chillcott of the University of New South Wales for many helpful comments and a critical reading of the manuscript. We are also grateful to Dr. Anne S. Ulrich for discussing with us her data on gramicidin S insertion prior to publication. We finally wish to express our gratitude to one of the referees for directing our attention to the endotoxin and pardaxin data, which we used in the Results section.

T.H. was supported by grant He1829/6-1 from the Deutsche Forschungsgemeinschaft.

REFERENCES

Bechinger, B., L. M. Gierasch, M. Montal, M. Zasloff, and S. J. Opella. 1996. Orientations of helical peptides in membrane bilayers by solid state NMR spectroscopy. *Solid State Nucl. Magn. Reson.* 7:185–191.

Bechinger, B. 1999. The structure, dynamics and orientation of antimicrobial peptides in membranes by multidimensional solid-state NMR spectroscopy. *Biochim. Biophys. Acta.* 1462:157–183.

Chatelier, R. C., and A. P. Minton. 1996. Adsorption of globular proteins on locally planar surfaces—models for the effect of excluded surface area and aggregation of adsorbed protein on adsorption equilibria. *Biophys. J.* 71:2367–2374.

Dan, N., and Safran, S. A. 1998. Effect of lipid characteristics on the structure of transmembrane proteins. *Biophys. J.* 75:1410–1414.

Ducarme, P., M. Rahman, and R. Brasseur. 1998. Impala—A simple restraint field to simulate the biological membrane in molecular structure studies. *Proteins Struct. Funct. Genet.* 30:357–371.

Hartsel, S. C., C. Hatch, and W. Ayenew. 1993. How does amphotericin B work? studies on model membrane systems. *J. Lipid. Res.* 3:377–408.

Gazit, E., P. La Rocca, M. S. P. Sansom, and Y. Shai. 1998. The structure and organization within the membrane of the helices composing the pore-forming domain of *Bacillus thuringiensis* δ-endotoxin are consistent with an "umbrella" structure of the pore. *Proc. Natl. Acad. Sci. U.S.A.* 95:12289–12294.

Gennis, R. B. 1989. Biomembranes. Molecular structure and function. Springer, New York.

Heimburg, T., and R. L. Biltonen. 1994. The thermotropic behavior of dimyristoyl phos-phatidylglycerol and its interaction with cytochrome *c*. *Biochemistry.* 33:9477–9488.

Heimburg, T., and D. Marsh. 1995. Protein surface-distribution and protein–protein interactions in the binding of peripheral proteins to charged lipid membranes. *Biophys. J.* 68:536–546.

Heimburg, T., B. Angerstein, and D. Marsh. 1999. Binding of peripheral proteins to mixed lipid membranes: effect of lipid demixing upon binding. *Biophys. J.* 76:2575–2586.

Kessel, A., D. S. Cafiso, and N. Ben-Tal. 2000. Continuum solvent model calculations of alamethicin–membrane interactions: Thermodynamic aspects. *Biophys. J.* 78:571–583.

Ladokhin, A. S., M. E. Selsted, and S. H. White. 1997. Sizing membrane pores in lipid vesicles by leakage of co-encapsulated markers–pore formation by melittin. *Biophys. J.* 72:1762–1766.

Minton, A. P. 1999. Adsorption of globular proteins on locally planar surfaces. II. Models for the effect of multiple adsorbate configurations on adsorption equilibria and kinetics. *Biophys. J.* 76:176–187.

Ohki, S., E. Marcus, D. K. Sukumaran, and K. Arnold. 1994. Interaction of melittin with lipid membranes. *Biochim. Biophys. Acta.* 1194:223–232.

Ojcius, D. M., and J. D. Young. 1991. Cytolytic pore-forming proteins and peptides: is there a common structural motif? *Trends Biochem. Sci.* 16:225–229.

Pramanik, A., P. Thyberg, and R. Rigler. 2000. Molecular interactions of peptide with phospholipid vesicle membranes as studied by fluorescence correlation spectroscopy. *Chem. Phys. Lipids* 104:35–47.

Rapaport, D., and Y. Shai. 1991. Interaction of fluorescently labeled pardaxin and its analogues with lipid bilayers. *J. Biol. Chem.* 266: 23769–23775.

Salgado, J., S. L. Grage, L. H. Kondejewski, R. N. McElhaney, and A. S. Ulrich. 2000. Interaction of Gramicidin S with synthetic lipid membranes: a ^{19}F Solid-State NMR study on oriented DMPC bilayers (presented at the International Bunsen Discussion Meeting on "Interaction of Biopolymers with Model Membranes" in Halle, Germany, March 2000).

Shai, Y. 1999. Mechanism of the binding, insertion and destabilization of phospholipid bilayer membranes by α-helical antimicrobial and cell nonselective membrane-lytic peptides. *Biochim. Biophys. Acta.* 1462:55–70.

Shillcock, J. C., and D. H. Boal. 1996. Entropy-driven instability and rupture of fluid membranes. *Biophys. J.* 71:317–326.

Talbot, J. 1997. Molecular thermodynamics of binary mixture adsorption: a scaled particle theory approach. *J. Chem. Phys.* 106:4696–4706.

Vaz Gomes, A., A. de Waal, J. A. Berden, and H. V. Westerhoff. 1993. Electric potentiation, cooperativity, and synergism of magainin peptides in protein-free liposomes. *Biochemistry.* 32:5365–5372.

Yang, L., T. M. Weiss, R. I. Lehrer, and H. W. Huang. 2000. Crystallization of antimicrobial pores in membranes: magainin and protegrin. *Biophys. J.* 79:2002–2009.